Comparative Analysis of Dual Source DC/DC converter Topologies for Improved Performance in Integration of Hybrid Energy Sources

Hamsavarthini Yoganandan*, Kanthalakshmi Srinivasan**

** Department of Electrical and Electronics Engineering,*
PSG College of Technology, Coimbatore, Tamil nadu, India-641004. (e-mail: 1907re01@psgtech.ac.in)
***Department of Electrical and Electronics Engineering,*
PSG College of Technology, Coimbatore, Tamil nadu, India-641004. (e-mail: skl.eee@psgtech.ac.in)

Abstract: Hybrid Energy Source is used to combine the multiple energy source, in order to use their characteristics at their best. A power electronic converter is needed to interface these hybrid energy source with a load. In traditional methods various single input DC-DC power electronic converters are used but it has drawbacks such as, complex design, huge cost and less efficiency. Therefore, it is important to identify the opportunities to cut down the cost and to enhance the performance of the converter. One such possibility is to use dual source DC-DC converter that leads to reductions of filter size, cost and losses. Taking this into consideration, this study explores, the detailed software simulation of three different topologies of dual source DC-DC converters (Topology-I, Topology-II and Topology-III) in MATLAB/Simulink platform. All the three converters can work in buck, boost and bidirectional mode. Furthermore, a performance comparison of these converter topologies are made to check the feasible converter for electric vehicle application. The performance comparison shows that the Topology-III converters has less component count, improved efficiency, high voltage gain, high average output power and compact structure when compared with existing converter topology (I and II).

Keywords: Bidirectional power flow; DC-DC power converters; Hybrid energy source; Topologies; Performance comparison

1. INTRODUCTION

Hybrid Energy Sources (HES) is one of the emerging technologies to integrate the energy sources that has diverse V-I characteristics such as wind, solar PV, battery, super capacitor etc. As per typical methods, the energy sources are combined using multiple single input DC-DC converters to a common DC link. However, the specific use of energy is not taken in to account due to their extremely inconsistent nature. Therefore, by combining two-energy source is brought into practice which is called hybridization. This energy system has earned more popularity because of its reliability and dynamic in operation when compared with single source. Hybrid Energy Sources primarily lean on power electronic converter to integrate energy sources. The power modulator used in the study is non-isolated dual source DC/DC converter.

A unique multiple input DC/DC converter was introduced (Kumar and Jain, 2013) with bidirectional capabilities and small signal modelling; power management control is validated in simulation and through experimental results. A novel Bidirectional DC-DC Converter (BDC), Improved Bidirectional DC-DC Converter (IBDC) converters, dual input and modified dual input DC-DC converter - analysis, circuit diagrams, working description, control strategy followed by topological comparison with other converters is carried out both in hardware and software (Athikkal et al.,2017a and Athikkal et al.,2017b). Simulation Vs experimental results comparison for three input DC-DC converter is carried out to check the performance and efficiency of the converter under different loading condition (Sivaprasad et al., 2015).

A detailed investigation on different configuration of multiple input DC-DC converter for hybrid electric vehicles is reported (Jyotheeswara Reddy and Natarajan, 2018). Multiple Input Single Output boost converter is designed and their working modes, small signal modelling analysis is carried out. A prototype circuit is developed, and justified with simulation (Mudadla Dhananjaya, 2019).

The proposed converter is compared with the existing converter in terms of component count, compact structure and efficiency. Further the simulation results are validated with experimental results (Kumaravel et al., 2018). A two input, two output DC-DC converter used to integrate different energy sources to provide a power to electric vehicle is verified with prototype (Kumaravel et al., 2019). Dual Input DC/DC converter and their architecture, conduction states of converter and its implementation in both software and hardware were presented (Kumar and Jain, 2012).

Simulation Vs experimental results comparison for three input DC-DC converter is carried out to check the performance and efficiency of the converter under different loading condition (Athikkal, 2020). A novel topology is developed to overcome the demerits of huge size, complexity in design and increased cost in traditional converter with single source supply (Sathishkumar et al., 2017). Dual input DC-DC Converter, Bridge type Dual Input DC-DC converters are presented and a prototype of those converters is developed and it is correlated with simulation results for DC microgrid application (Athikkal et al., 2018). Dual input DC-DC converter with slighter modification in arrangement is preferred, Software simulation is conducted and results are elaborated in detail. A standard prototype is built to match with the computer model (Athikkal et al., 2017c). A SEPIC configuration with dual input DC-DC converter topology is simulated and a hardware model is developed to check the converter capability (Yasin et al., 2019).

The proposed topology offers good accuracy, simple in control and durable in voltage source selection. An extensive comparison of the converter with current literature is presented and it simulated in MATLAB/ SIMULINK, further verified with digital controller (Thakur and Patel, 2019). This study is carried to provide an investigation on multi-input DC-DC converters for electric vehicle systems (Affam et al., 2021). Different DC-DC converter topologies for electric vehicles is presented, analyzed and compared in detail (Chakraborty et al., 2019). A dual input super boost DC-DC converter for electric vehicle application is designed and validated with simulation and hardware results (Kumar et al., 2019).

A step-up multi-input DC-DC converter, multi-input multi-output DC-DC boost converter and dual active bridge DC-DC converter for electric vehicle application is designed and verified with experimental results (Ahrabi et al., 2017; Karthikeyan and Gupta, 2018).

A fast voltage loop's stability analysis and design of DC-DC converters based on the Popov criterion is discussed in detail. It interconnects the nonlinear system with linear system (Petru Dobra et al., 2007).

An optimization technique is incorporated in order to improve the stability and performance of the closed loop DC-DC Switched Mode Boost Converter. Further, the closed loop control is implemented in the dSPACE, and the performance of the converter is compared with conventional controller and also with the optimized Type II/Type III controllers (Arnab Ghosh and Subrata Banerjee, 2015).

A step-by-step procedure is followed to create a state feedback controller for an DC-DC buck converter circuit in order to track the output-voltage (Omer Saleem Bhatti, et al., 2018). The buck converters output voltage is regulated using Proportional-Integral-Derivative controller along with a Linear - Quadratic - Regulator (Omer Saleem Bhatti, et al., 2019).

A Sliding Mode Controller is proposed for power factor correction in Bridgeless Interleaved Boost Converter (Subashini et al., 2019). Adaptive neuro-fuzzy inference system controller based on high Gain DC-DC converter is designed and developed for energy harvesting application (Marikkannan et al., 2019). The voltage source converter is controlled by using a super-twisting sliding mode predictive current control. The energy required for a micro-grid is supplied by using the battery, PV and wind energy (Ridha Benadli, 2019).

Hybrid power system is controlled by using an Integral sliding mode controller and PI controller (Masoud Bahmanpour et al., 2019). A PI controller is used to control the quadratic boost converter with an energy source as battery and solar panel (Dhanaraj Amudhavalli, 2020). Chaos and Bifurcation analysis is carried out in Continuous input and output power boost converter using Average Current Mode (ACM) controller and General Pulse Width Modulation (GPWM) controller (Maheswari Ellappan et al., 2020).

2. GENERAL BLOCK DIAGRAM OF DUAL SOURCE DC-DC CONVERTER

A general form of two input DC/DC Converter is conceptually represented in Fig. 1.

The sources will provide energy depending upon the load demand. The power is transferred from one end to another end through DC-DC converter. By proper tuning of duty cycle, the converter will buck and boost the voltage level.

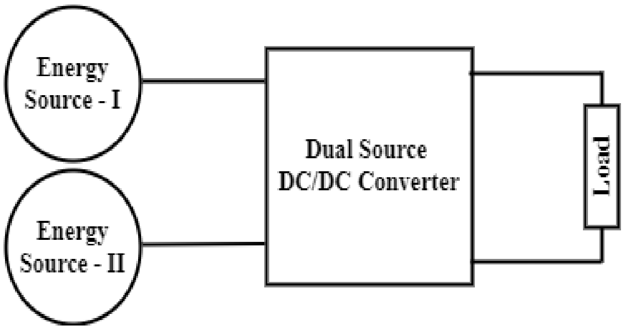

Fig. 1. Block diagram of dual source DC-DC converter.

3. TOPOLOGICAL COMPARISON OF DIFFERENT DUAL INPUT CONVERTER

3.1. Multiple input non isolated DC/DC converter (Topology-I):

Architecture of Multiple input non isolated DC/DC converter is shown in Fig. 2.

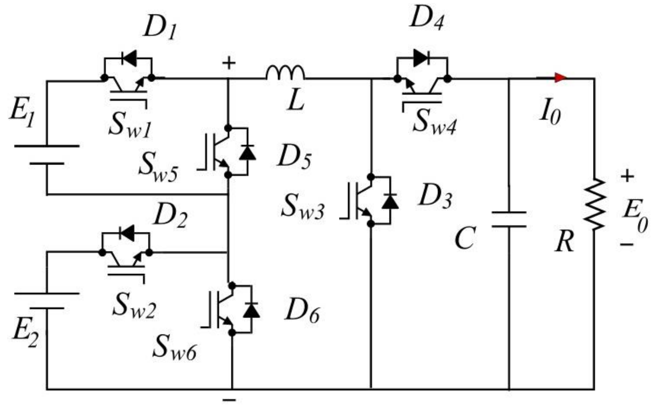

Fig. 2. Multiple input non-isolated DC-DC converter (Topology-I).

The pulsating voltage source are represented with the E_1 and E_2, S_{W1}, S_{W2}, S_{W3}, S_{W4}, S_{W5}, S_{W6} switches, followed by D_1, D_2, D_3, D_4, D_5 and D_6 diodes. The switch S_{W1} and S_{W2} determine the conduction and supply sources while the switches S_{W3} decides the converter mode under buck, boost. S_{W4}, S_{W5} and S_{W6} decides the bidirectional mode [1].

Fundamental waveform of voltage and current through the inductor during various working state of the Topology-I over one revolution (unidirectional mode) is shown in Fig. 3. The Topology-I waveform under bidirectional mode is given in Fig. 4.

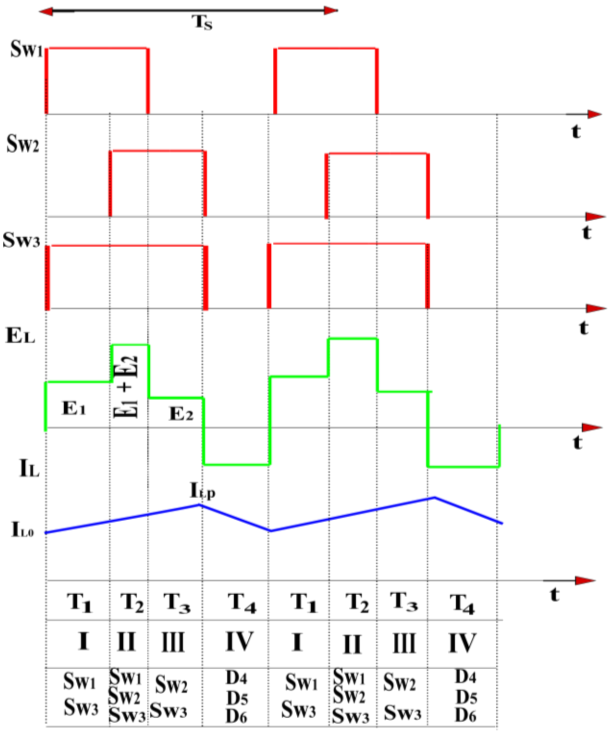

Fig. 3. Operating waveform of Topology-I (Source to Load)

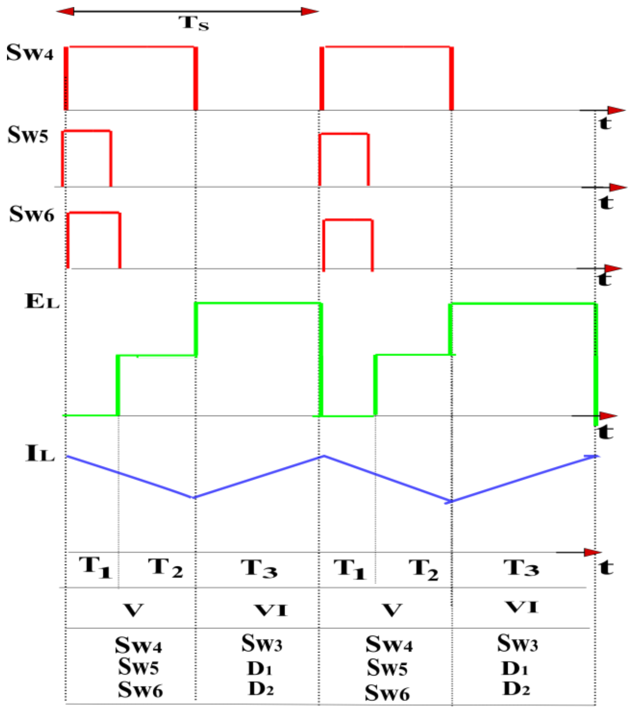

Fig. 4. Operating waveform of Topology-I (Load to Source).

Operating modes of Topology-I and their analytical waveforms is shown in Table 1.

Table 1. Various working modes of Topology-I.

Working modes (Unidirectional)	Supplying Source	ON state switch	Inductor voltage	Inductor status
Working mode-I	E_1	Sw_1, Sw_3	$E_1 - E_0$	charging
Working mode-II	E_1+E_2	Sw_1, Sw_2, Sw_3	E_1+E_2-E_0	charging
Working mode-III	E_2	Sw_2, Sw_3	E_2-E_0	charging
Working mode-IV	None	D_4, D_5, D_6	-E_0	discharging
Working modes (Bidirectional)	Receiving Source	ON state switch	Inductor voltage	Inductor status
Working mode-V	-E_O	Sw_4, Sw_5, Sw_6	-E_O	charging
Working mode-VI	E_1+E_2	Sw_3, D_1, D_2	E_1+E_2	discharging

Simulation parameters considered for Topology-I are discussed in Table 2.

Table 2. Simulation parameters of Topology-I.

S. No	Parameters	Specification in Boost Mode	Specification in Buck Mode
1	Input Source voltage-(E_1)	24 V	
2	Input Source voltage-(E_2)	12 V	
3	Duty ratio(d_1)	60%	40%
4	Duty ratio(d_3)	60%	0%
5	Duty ratio(d_2)	60%	40%
6	Inductor(L)	14.4mH	
7	Capacitor(C)	216μF	
8	Switching Frequency (F_S)	10kHz	
9	load resistance(R)	10Ω	
10	Output voltage (E_O)	53.3 V	13.7 V

Output equation of buck mode converter is

$$E_o = E_1 d_1 + E_2 d_2 \tag{1}$$

Output equation of boost mode converter is

$$E_o = \frac{E_1 d_1 + E_2 d_2}{(1 - d_3)} \tag{2}$$

3.2. Improved Bridge Type Dual Input DC-DC (IBDC) Converter (Topology-II):

Topology-II consists of six switches (Sw_1, Sw_2, Sw_3, Sw_4, Sw_5, Sw_6) and there are four diodes (D_3, D_4, D_5 and D_6) only for the switches (Sw_3, Sw_4, Sw_5 and Sw_6) along with bidirectional capabilities as shown in Fig.5. The power will be delivered to the load from individual energy sources/simultaneous energy sources. And it has compact structure with good efficiency in loading condition [2-3].

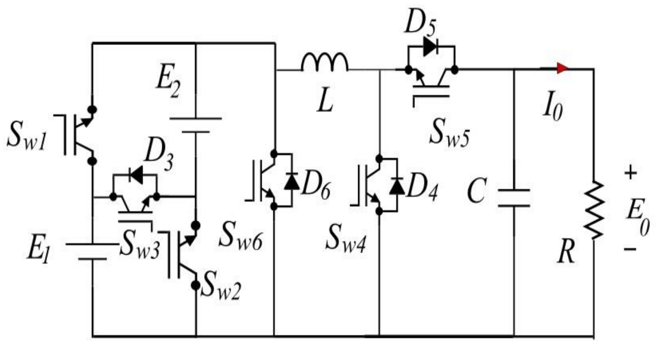

Fig. 5. Improved bridge type dual input DC-DC converter (Topology-II).

Steady state waveforms of a Topology-II under unidirectional state over a one cycle is shown in Fig.6. Switching signal of switches, inductor voltage and current waveform under bidirectional state is shown in Fig.7.

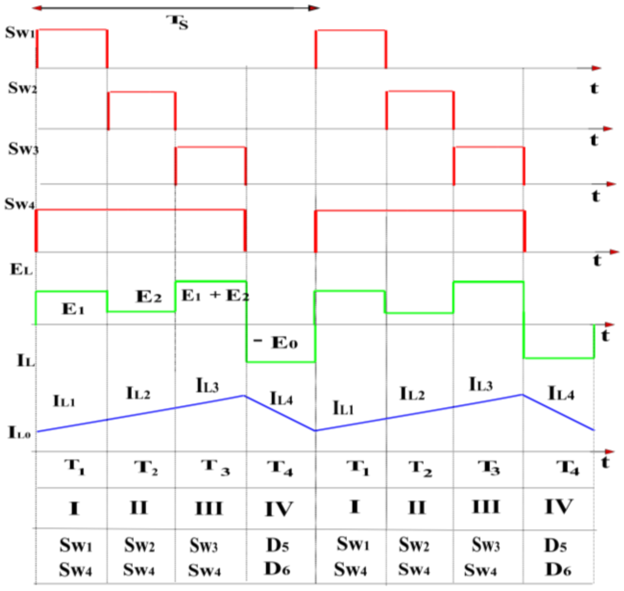

Fig. 6. Typical waveform of Topology-II (Source to Load).

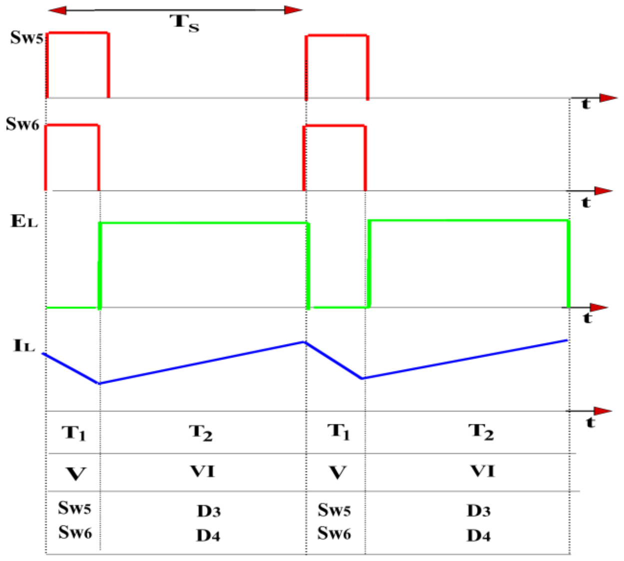

Fig. 7. Typical waveform of Topology-II (Load to Source).

Possible operating modes of Topology-II is shown in Table 3.

Table 3. Different working modes of Topology-II.

Working modes (Unidirectional)	Supplying Source	ON state switch	Inductor voltage	Inductor status
Working mode-I	E_1	S_{W1}, S_{W4}	$E_1 - E_0$	charging
Working mode-II	E_2	S_{W2}, S_{W4}	E_2-E_0	charging
Working mode-III	E_1+E_2	S_{W3}, S_{W4}	E_1+E_2-E_0	charging
Working mode-IV	None	D_5, D_6	-E_0	discharging
Working modes (Bidirectional)	**Receiving Source**	**ON state switch**	**Inductor voltage**	**Inductor status**
Working mode-V	-E_O	S_{W5}, S_{W6}	-E_O	charging
Working mode-VI	E_1+E_2	D_3, D_4	E_1+E_2	discharging

After the various working modes of the Topology-II, followed by the parameters considered for the simulation of Topology-II is shown in Table 4.

Table 4. Simulation parameters of Topology-II.

S. No	Parameters	Specification in Boost Mode	Specification in Buck Mode
1	Input Source voltage-(E_1)	50 V	
2	Input Source voltage-(E_2)	30 V	
3	Duty ratio(d_1)	-	15%
4	Duty ratio(d_3)	Continuous on	10%
5	Duty ratio(d_2)	-	15%
6	Duty ratio(d_4)	20%	-
7	Inductor(L)	7mH	
8	Capacitor(C)	470µF	
9	Switching Frequency (F_S)	20kHz	
10	load resistance(R)	10Ω	
11	Output voltage (E_O)	100 V	20 V

Output equation of buck mode converter is

$$E_o = E_1 d_1 + E_2 d_2 + (E_1 + E_2) d_3 \tag{3}$$

Output equation of boost mode converter is

$$E_o = \frac{(E_1 + E_2)}{(1 - d_4)} \tag{4}$$

3.3 Enhanced dual source DC-DC converter (Topology- III):

The switches are operated in appropriate manner in order to send power as well as receive power as shown in Fig.8. Here, the common inductor shares the sources. Anyone of the switches S_{W1} /S_{W2} / S_{W3} / diode D_4 will conduct at a time. There only diodes D_3 and D_4 for the switches S_{W3} and S_{W4}. By altering the duty cycle of semiconductor switches S_{W1}, S_{W2}, S_{W3} and S_{W4} the power continues to flow from / to source is controlled.

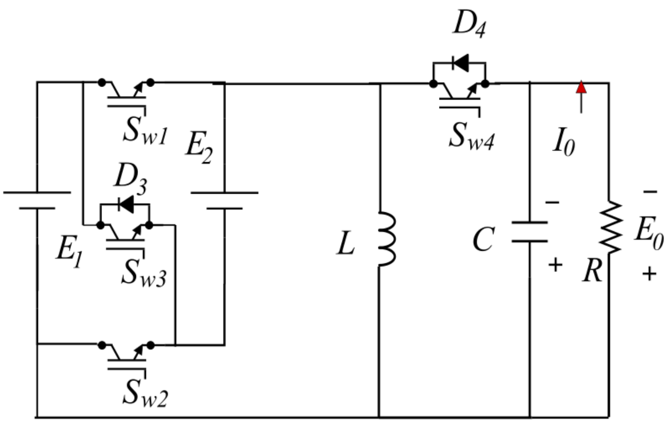

Fig. 8. Enhanced dual source DC/DC converter (Topology-III).

The Topology-III is operated in Modes 1-4 under unidirectional mode. Similarly, it operates in two more Modes 5 and 6 under bidirectional mode. The waveforms of Topology-III in stable condition under unidirectional mode are given in Fig.9. The waveforms of the Topology-III under bi-directional mode over one cycle as shown in Fig.10.

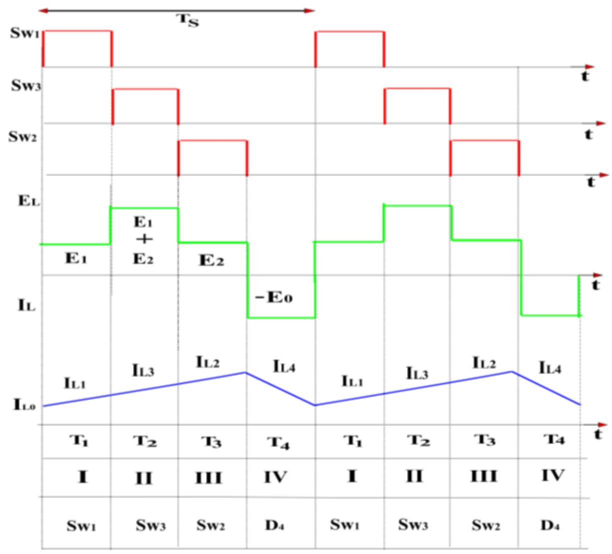

Fig. 9. Analytical waveform of Topology-III (Source to load).

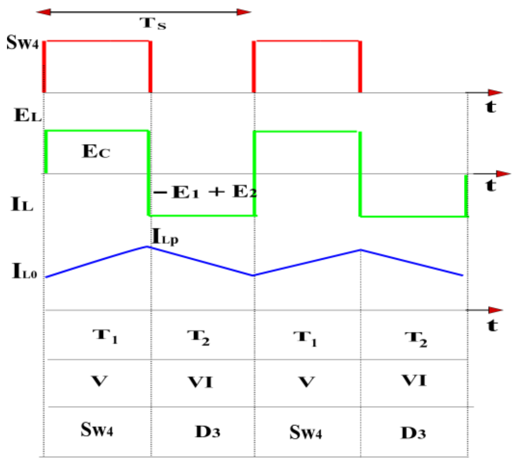

Fig. 10. Analytical waveform of Topology-III (Load to Source).

The unidirectional and bidirectional operating modes of Topology-III is shown in Table 5 followed by the discussion about the simulation parameters.

Table 5. Different working modes of Topology-III.

Working modes (Unidirectional)	Supplying Source	ON state switch	Inductor voltage	Inductor status
Working mode-I	E_1	S_{W1}	$E_1 - E_0$	charging
Working mode-II	E_1+E_2	S_{W3}	$E_1+E_2-E_0$	charging
Working mode-III	E_2	S_{W2}	E_2-E_0	charging
Working mode-IV	None	D_4	$-E_0$	discharging
Working modes (Bidirectional)	**Receiving Source**	**ON state switch**	**Inductor voltage**	**Inductor status**
Working mode-V	$-E_O$	S_{W4}	$-E_O$	charging
Working mode-VI	E_1+E_2	D_3	E_1+E_2	discharging

Parameters considered for simulation of Topology-III as shown in Table 6. Topology – III will able to produce a high boost in output voltage due to the simultaneous operation of both the energy sources by using switch (S_{W3}).

Table 6. Simulation parameters of Topology-III.

S. No	Parameters	Specification in Boost Mode	Specification in Buck Mode
1	Input Source voltage-(E_1)	48 V	
2	Input Source voltage-(E_2)	36 V	
3	Duty ratio(d_1)	20%	15%
4	Duty ratio(d_3)	32.5%	10%
5	Duty ratio(d_2)	20%	15%
6	Inductor(L)	6.5mH	
7	Capacitor(C)	433μF	
8	Switching Frequency (F_S)	10kHz	
9	load resistance(R)	160Ω	
10	Output voltage (E_O)	-160 V	-35V

Output equation of buck and boost mode converter is given by

$$E_o = -\left(\frac{E_1 d_1 + (E_1 + E_2) d_3 + E_2 d_2}{1 - (d_1 + d_2 + d_3)}\right) \tag{5}$$

4. SIMULATION RESULTS AND DISCUSSION

4.1. Simulation results of Topology-I

4.1.1 Boost Mode:

Input voltage and switching signals are given to switches S_{W1}, S_{W2}, S_{W3} are represented in Table 2 followed by the initial voltage over the inductor is 12 V (i.e., E_1 - E_O). Further, charged inductor has a voltage of (E_1 + E_2 - E_O), i.e., 36 V and the voltage of inductor is discharged to 30 V (E_O) for the remaining duration is shown in Fig.11(a) and inductor current is charged to 13.18 A and discharged to 13.10 A as shown in Fig.11(b). The voltage across the resistor is of 52.06 V and output current is of 5.206 A and it is shown in Fig.11(c) and Fig.11(d).

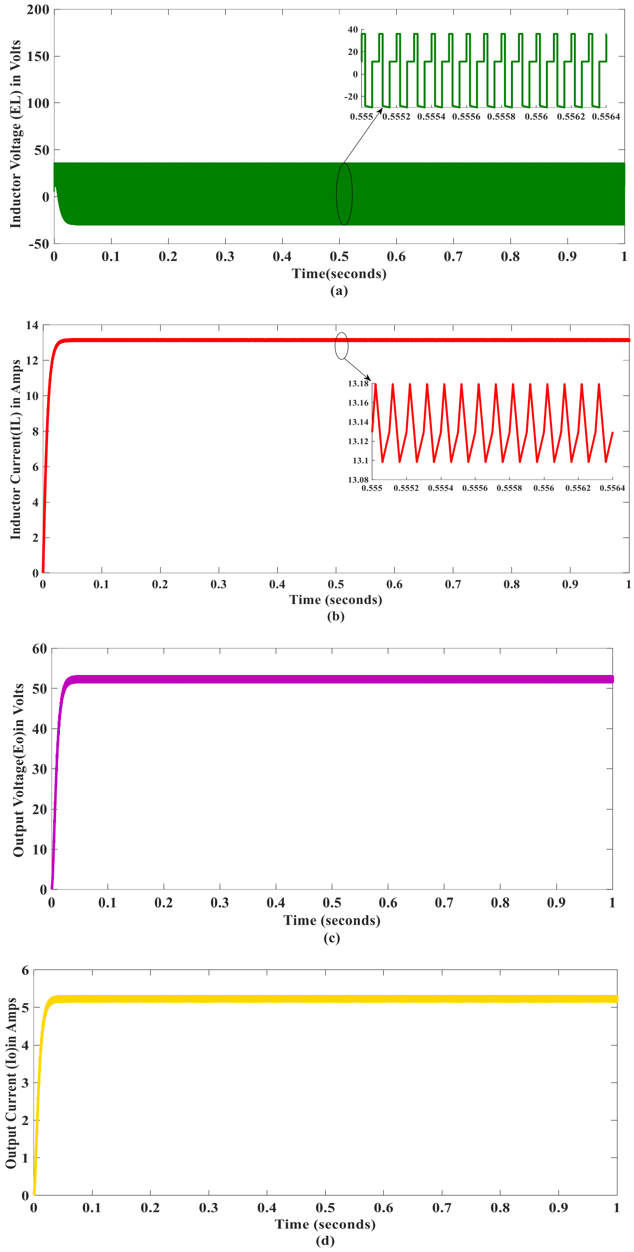

Fig. 11. (a) Inductor voltage (b) Inductor current (c) Output voltage (d) Output current of Topology-I [d_1=0.6, d_2=0.6, d_3=0.6, E_1=24 V, E_2=12 V, E_O=52.06 V, I_O=5.206 A].

4.1.2 Buck Mode:

The input voltage and switching signals given to the switches S_{W1}, S_{W2} is shown in Table 2. At time (t_1), inductor voltage is of 10 V (i.e., E_1 - E_O). and for time (t_2), the inductor charges to a 22 V (i.e., E_1 + E_2 - E_O), for time (t_3), inductor discharged to 2.5 V (i.e., E_1 - E_O) while at time (t_4) further the inductor current is discharged to its initial position Fig.12(a) and inductor current is charged to 1.364 A and discharged to 1.32 A as shown in Fig. 12(b). By varying the duty cycles d_1 and d_2, the inductor current, load current and the output voltage can be controlled. The output voltage is of 13.44 V and the output current is of 1.344 A as shown in Fig.12(c) and Fig.12(d).

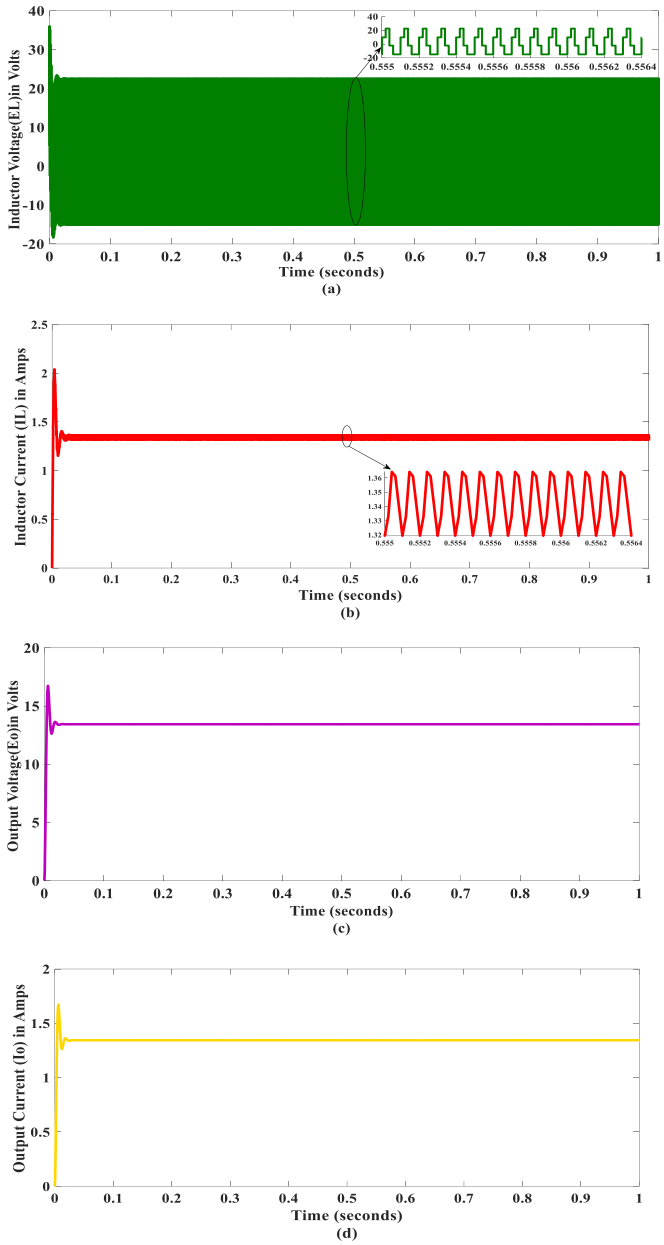

Fig. 12. (a) Inductor voltage (b) Inductor current (c) Output voltage (d) Output current of Topology-I [d_1=0.4, d_2=0.4, E_1=24 V, E_2=12 V, E_O=13.44 V, I_O=1.344 A].

4.1.3 Bidirectional Mode:

The bidirectional operation of Topology-I is justified, by considering an input voltage of E_{in} =30 V. The switching signals are given to switches S_{W4}, S_{W5}, S_{W6} with duty ratio d_4= 52% d_5=20% d_6=20% respectively. An inductor is charged to voltage of 20 V, initially it is discharged to -10 V and finally it is discharged to -30 V is shown in Fig.13(a) and an inductor current is charged to -2.15 A and discharged to -2.21 A as shown in Fig.13(b). The output voltage yielded by the Topology-I is 19.14 V (E_{O1}+E_{O2}) as shown in Fig.13(c) and output current is 4.29 A is shown in Fig.13(d) as the Topology-I works as single input multiple output converter.

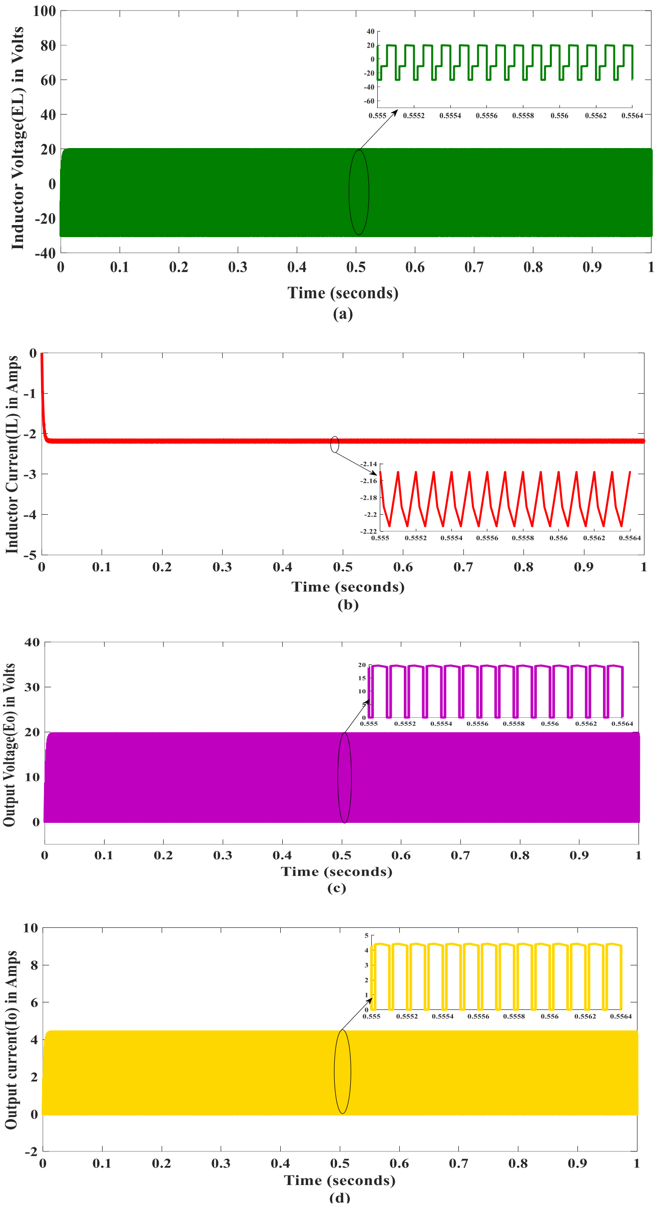

Fig. 13. (a) Inductor voltage (b) Inductor current (c) Output voltage (d) Output current of Topology-I [d_4=0.52, d_5=0.2, d_6=0.2, E_{in}=30 V, E_L=19.13V, I_L=-2.15A, E_{O1}=10.75V, E_{O2}=8.38V, E_{O1}+E_{O2}=E_O =19.14 V, I_O=4.29A].

4.2. *Simulation results of Topology-II*

4.2.1 Boost Mode:

Input voltage and switching signal S_{W3} and S_{W4} is given to the Topology-II is shown in Table 4. For simple operation consider series connection switch S_{W3} between E_1 and E_2 and it is turned ON permanently, while S_{W1} and S_{W2} are turned off and S_{W3} charges the inductor by two inputs together with a voltage of 80 V (i.e., E_1 + E_2) is shown in Fig.14(a). Inductor current is charged to 12.54 A and discharged to 12.42 A as shown in Fig.14(b). Finally, the inductor is discharged to a voltage is -20 V (i.e., E_1 + E_2 - E_O). As shown in Fig.14(c) and Fig.14(d), the output voltage and output current across the resistor is 99.97 V and 9.997 A.

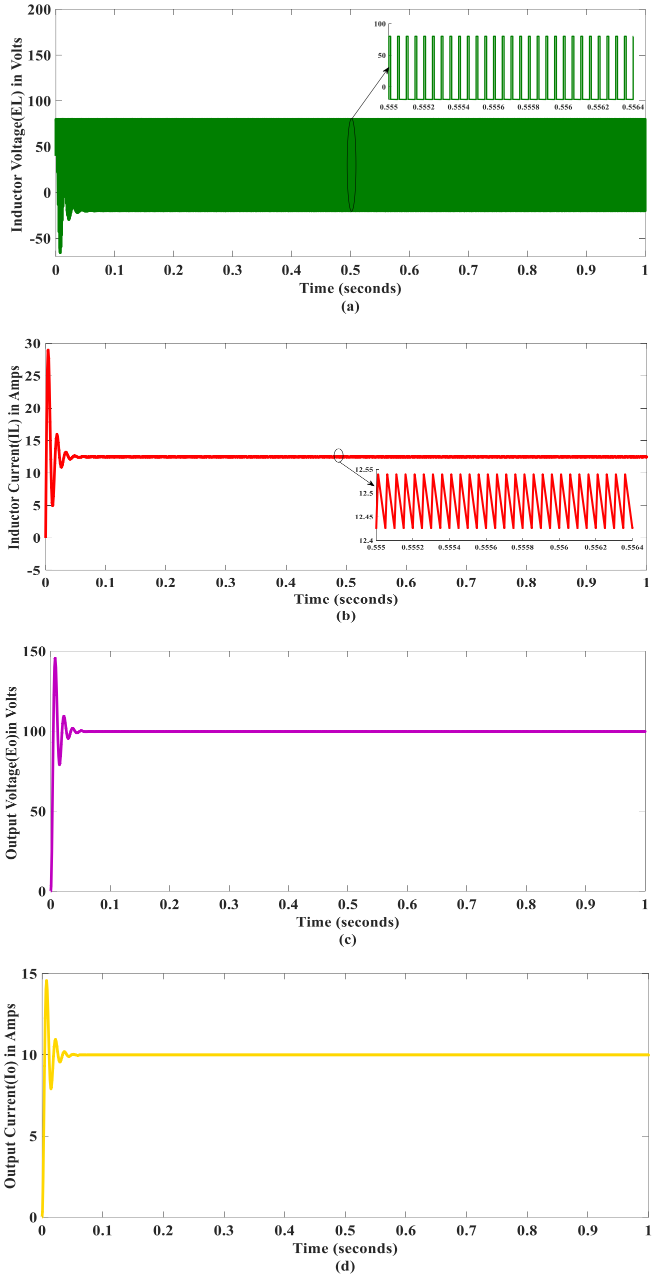

Fig. 14. (a) Inductor voltage (b) Inductor current (c) Output voltage (d) Output current of Topology-II [d_3=Continuous 'on', d_4=0.2, E_1=50 V, E_2=30 V, E_O=99.97 V, I_O=9.997 A].

4.2.2 Buck Mode:

Input voltage and switching signal S_{W1}, S_{W2}, S_{W3} is given to the Topology-II is shown in Table 4. The inductor charges to 30 V (i.e., E_1-E_O) for d_1 duty ratio, 10 V (i.e., E_2-E_O) for d_2 duty ratio and 60 V (i.e., E_1+ E_2-E_O) for duty ratio d_3, at last, the inductor is discharging to a voltage of -19.54 V (i.e., -E_O) is shown in Fig.15(a) and inductor current is charged to 1.99 A and discharged to 1.91 A for the remaining period as shown in Fig.15(b). The output voltage and output current is settled down to a value of 19.54 V and 1.91 A as shown in Fig.15(c) and 15 (d).

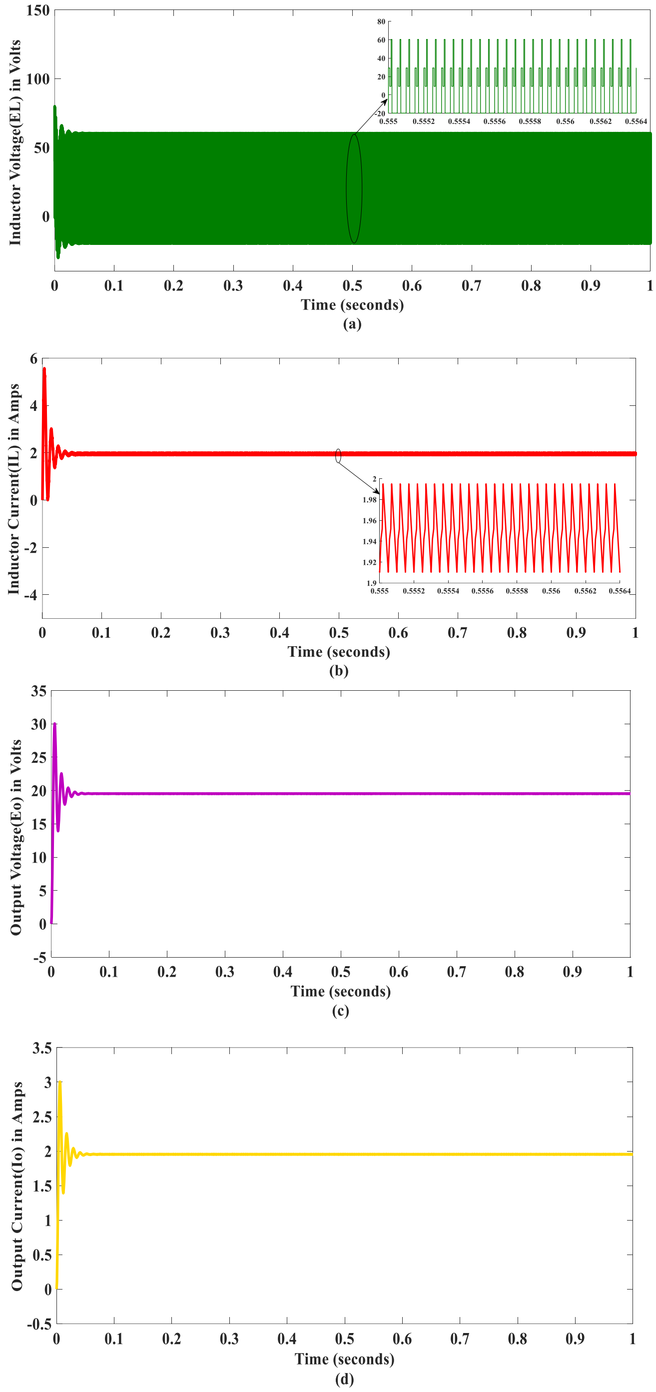

Fig. 15. (a) Inductor voltage (b) Inductor current (c) Output voltage (d) Output current of Topology- II [d_1=0.15, d_2=0.15, d_3=0.1, E_1=50 V, E_2=30 V, E_O=19.54 V, I_O=1.91 A].

4.2.3 *Bidirectional Mode (Buck Mode):*

The bidirectional operation is verified with an input voltage of E_{in} = 30 V. Switching signals are given to switches S_{W5}, S_{W6} with duty ratio d_5= 20% and d_6= 20%. The inductor charges to a 7.4 V and finally it is discharged to -30 V is shown in Fig.16(a) and inductor current is charged to -14.92 A and discharged to -14.96 A as shown in Fig.16(b). The converter gives an output voltage of 14.92 V (E_{O1}+E_{O2}) is shown in Fig.16(c) and output currentof 14.9 A is shown in Fig.16(d).

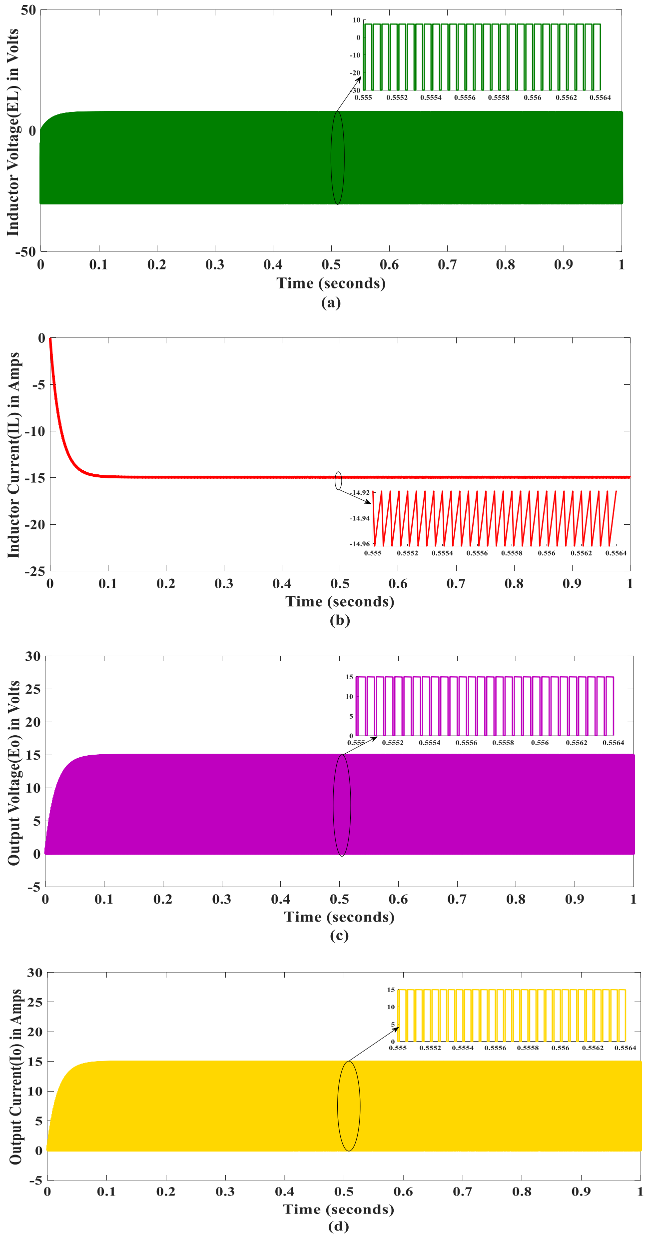

Fig. 16. (a) Inductor voltage (b) Inductor current (c) Output voltage (d) Output current of Topology-II [d_5= 0.2, d_6=0.2, E_{in}=30 V, E_L=7.482 V, I_L=-14.92 A, E_{O1}=7.459 V, E_{O2}=7.459 V, E_{O1}+E_{O2}= E_O=14.92 V, I_O=14.9 A].

4.3. *Simulation results of Topology-III*

4.3.1 *Boost Mode:*

In boost mode input voltage and switching signal S_{W1}, S_{W2}, S_{W3} is given to the Topology-III is shown in Table 6. For d_1 the voltage over the inductor is 48 V (i.e., E_1 - E_O), and the inductor charges to a voltage of (E_1 + E_2 - E_O), i.e., 84 V for d_3. Further inductor discharges to a 36 V (i.e., E_2 -E_O) for d_2 and it is finally discharged to a (-E_O) i.e., - 159 V, for the remaining time period is shown in Fig.17(a) and an inductor current is charged to 4.57 A and discharged to 3.9 A as shown in Fig.17(b). The output voltage is of - 159 V and output current is of - 0.9937 A is shown in Fig.17(c) and Fig.17(d).

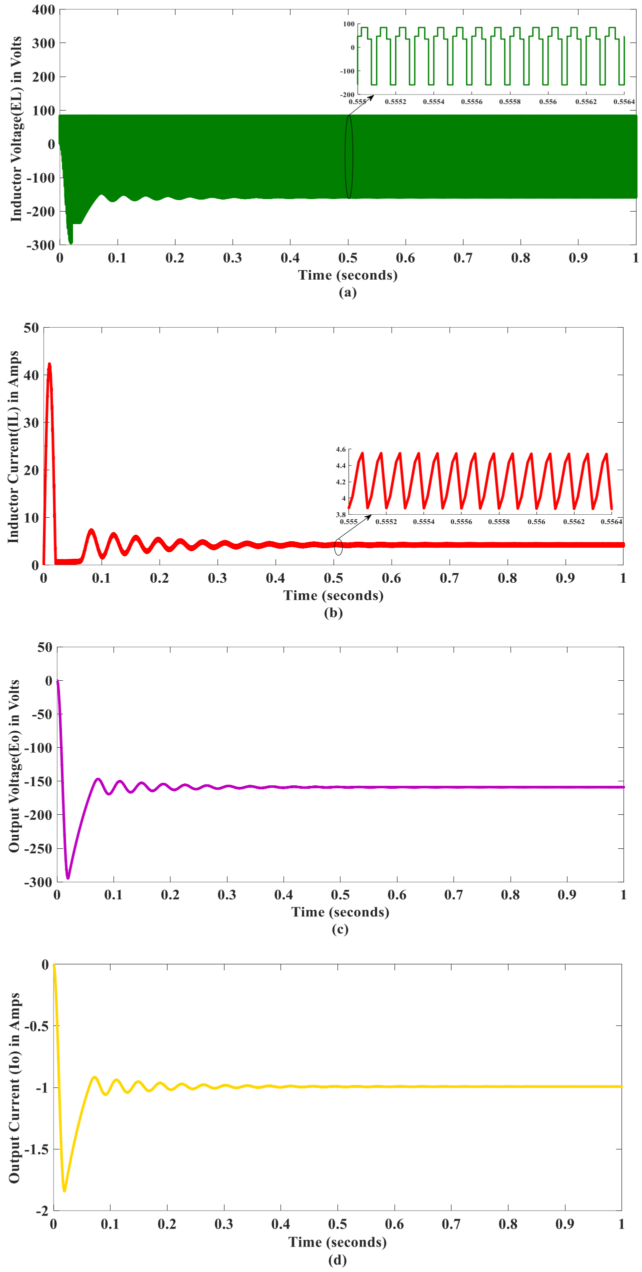

Fig. 17. (a) Inductor voltage (b) Inductor current (c) Output voltage (d) Output current of Topology- III [d_1=0.2, d_2=0.2, d_3=0.325, E_1=48 V, E_2=36 V, E_O= -159 V, I_O=-0.9937 A].

4.3.2 Buck Mode:

Input voltage and switching signal S_{W1}, S_{W2}, S_{W3} is given to the Topology -III is shown in Table 6. It is obvious that the inductor is charged to a 48 V (i.e., E_1-E_O) for d_1, 36 V (i.e., E_2-E_O) for d_2 and 84 V (i.e., E_1 + E_2 - E_O) for d_3. Finally, the inductor is discharged to a -34.52 V (i.e., - E_O) for the rest of the period is shown in Fig.18(a) and an inductor current is charged to 0.64 A and discharged to 0.33 A as shown in Fig.18(b). The output voltage and output current waveform reaches to a steady state value of -34.52 V and -0.2157 A is shown in Fig.18(c) and 18(d).

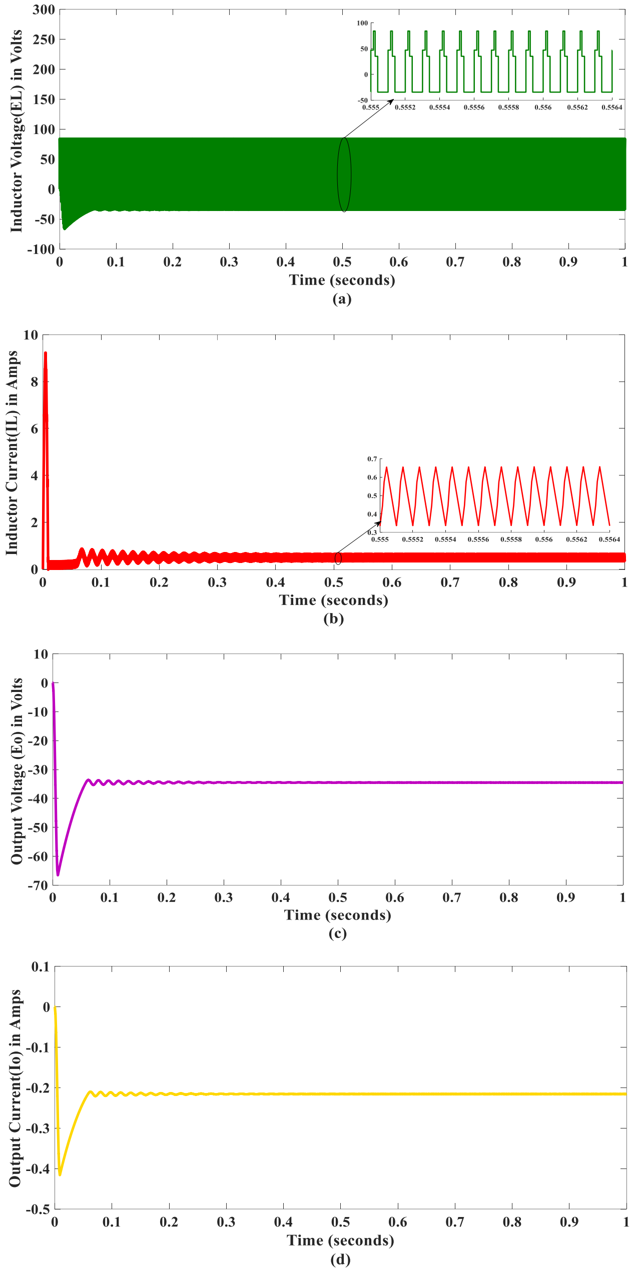

Fig. 18. (a) Inductor voltage (b) Inductor current (c) Output voltage (d) Output current of Topology-III [d_1=0.15, d_2=0.15, d_3=0.1, E_1=48 V, E_2=36 V, E_O=-34.52 V, I_O=-0.2157 A].

4.3.3 Bidirectional Mode:

The bidirectional working of Topology-III is considered with an input voltage of E_{in} =-160 V. Switching signals are given to switches S_{W4} with duty ratio d_4=34%. The inductor charges to 81.65 V and finally it is discharged to -160 V is shown in Fig.19(a). Inductor current is charged to -41.7 A and discharged to -40.92 A as shown in Fig.19(b). The output voltage of 81.65 V is produced by the Topology-III such as (E_{O1}+E_{O2}) is shown in Fig.19(c) and output current of 81.61 A is shown in Fig.19(d).

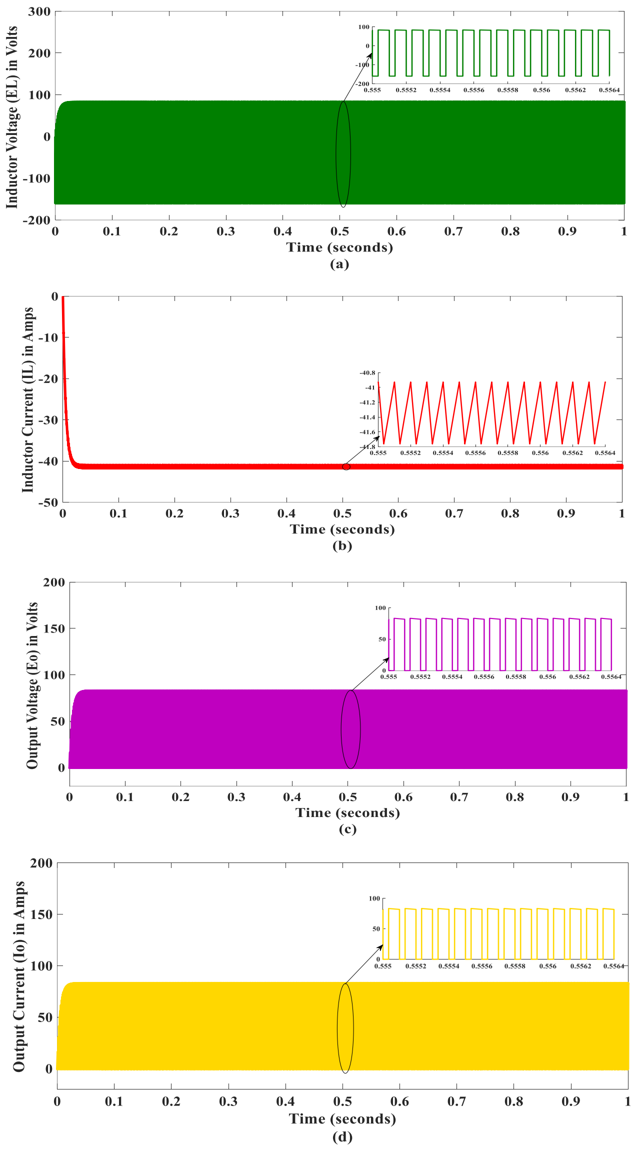

Fig. 19. (a) Inductor voltage (b) Inductor current (c) Output voltage (d) Output current of Topology-III [d_4= 0.34, E_{in}= -160 V, E_L=81.65 V, I_L=-40.93 A, E_{O1}=40.8 V, E_{O2}=40.8 V, $E_{O1}+E_{O2}$= E_O=81.65 V12, I_O=81.61 A].

4.4. Performance Comparison of Different Topologies

The three topologies are compared in terms of efficiency, output voltage, average output power are discussed in detail below

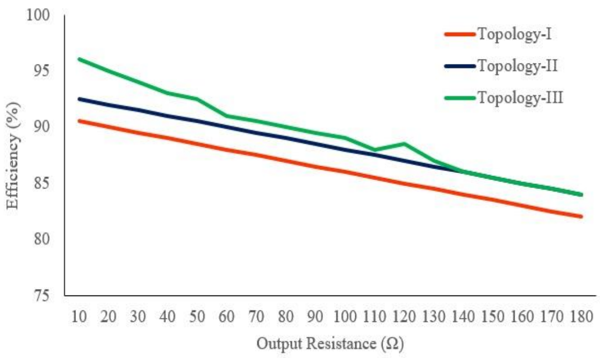

Fig. 20. Efficiency Vs Output Resistance.

The topologies are scaled down to E_1=48 V, E_2=36 V, and duty ratio for boost mode is taken for simulation. From the results, Topology-III provides better efficiency when compared with Topology-I and II and it is shown in Fig.20.

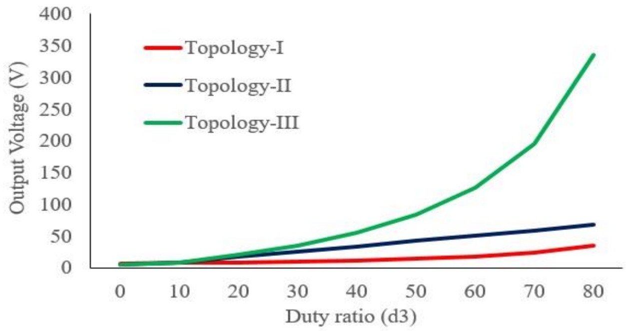

Fig. 21. Output voltage Vs Duty ratio (d_3).

The output voltage is compared with duty ratio as shown in Fig.21. To calculate an output voltage, three different topologies are scaled down to E_1=48 V, E_2=36 V, R=160 Ω, d_1 = 10% d_2 = 10% and d_3 is varied from 0% to 80%. The comparison proves that the Topology III provides a high output voltage than Topology-I and Topology-II.

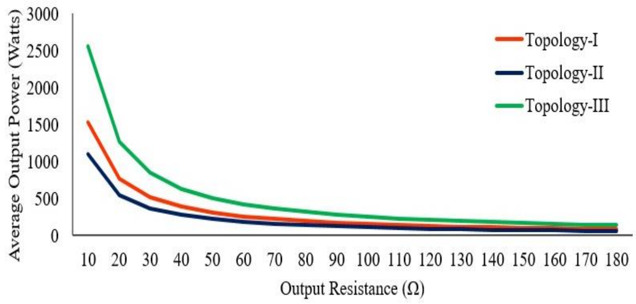

Fig. 22. Average output power Vs Output resistance.

The voltages of three different topologies are scaled down to E_1=48 V, E_2=36 V, and duty ratio for boost mode is taken for simulation from the simulation result, topology-III produces more average output power for change in load resistance as shown in Fig.22.

Table 7. Performance comparison.

Parameter	Topology-I	Topology-II	Topology-III
Inductor	1	1	1
Capacitor	1	1	1
IGBT'S	6	6	4
%Efficiency	82-91%	84-93%	84-96%

It is inferred that Topology-III gives a better efficiency with reduced no of switches compared with other topologies as discussed in Table 7.

5. CONCLUSION

Three types of non-isolated DC–DC converter to incorporate different sources such as, battery, wind, supercapacitor, solar and fuel cell etc. are reported. A multi input non-isolated DC/DC converter (Topology-I), An Improved bridge type dual input DC-DC converter (Topology-II) and an enhanced dual source DC-DC converter (Topology-III) with their mode of operation, steady state waveform for both unidirectional/bidirectional mode, design parameters and output equation of different modes are elaborated.

Later, the simulation results of buck, boost and bidirectional modes of all three topologies are presented in a sequential order.

Finally, a performance comparison is made by comparing the Topology –III with the existing Topology-I and Topology-II in terms of component count, efficiency, output voltage vs duty ratio and average output power vs output resistance. From the above results, the Topology-I has a voltage gain of 34.82 V with an efficiency of 91% and the average output power produced by the converter is 1.5kW. The Topology-II converter has a voltage gain of 67.08 V with an efficiency of 93% and the average output power is 1.1kW. The Topology-III, produces a voltage gain of 336 V with an efficiency of 96%, Further the average output power of Topology-III is 2.5 kW. It is concluded that the Topology-III can operate both in Unidirectional/ bidirectional mode with improved efficiency, and also it provides a high average output power, wide control range for output voltage with reduced no of switches. Hence, it is suitable for applications including electric vehicle and renewable energy sources.

REFERENCES

Affam, A., Buswig, YM., Othman, ABH., Bin Julai N., Qays O., (2021).A review of multiple input DC-DC converter topologies linked with hybrid electric vehicles and renewable energy systems.*Renewable and Sustainable. Energy Reviews,*135,1-23.

Ahrabi, R.R., Ardi, H., Elmi, M., Ajami, A., (2017).A novel step-up multi-input DC–DC converter for hybrid electric vehicles application.*IEEE Transactions on Power Electronics*,32(5),3549–3561.

Arnab Ghosh., Subrata Banerjee.,(2015).Control of Switched-Mode Boost Converter by using classical and optimized Type controllers.*Journal of Control Engineering and Applied Informatics*,17(4),114-125.

Athikkal, S., Kumar, G.G., Sundaramoorthy, K., Sankar, A., (2017a).Performance Analysis of Novel Bridge Type Dual Input DC-DC Converters. *IEEE Access*, 5,15340–15353.

Athikkal, S., Sundaramoorthy, K., Sankar, A., (2017b).Design, fabrication and performance analysis of a two input-single output DC-DC converter.*Energies*,10 (9),1-18.

Athikkal, S., Sundaramoorthy, K., Sankar, A., (2018). Development and performance analysis of dual input DC–DC converters for DC microgrid application.*IEEJ Transactions on Electrical and Electronics Engineering*, 13(7),1034–1043.

Athikkal, S., Sundaramoorthy, K., Sankar, A.,(2017c).A modified dual input dc-dc converter for hybrid energy application.*International Journal of Power Electronics and Drive System,*8(1),81–92.

Chakraborty, S., Vu, H., Hasan, M.M., Tran, D., El Baghdadi, M., Hegazy, O., (2019).DC-DC Converter Topologies for Electric Vehicles, Plug-in Hybrid Electric Vehicles and Fast Charging Stations: State of the Art and Future Trends.*Energies*,12(8),1-43.

Dhanaraj Amudhavalli., Nalin Kant Mohanty., (2020).Quadratic Boost Converter with integrated Energy Storage using PI controller for Low Power Photovoltaic Applications.*Journal of Control Engineering and Applied Informatics*,22(3),50-61.

Jyotheeswara, K. Reddy., Sudhakar Natarajan.,(2018). Energy sources and multi-input DC-DC converters used in hybrid electric vehicle applications-A review. *International Journal of Hydrogen Energy*,43(36), 17387–17408.

Karthikeyan, V., Gupta, R., (2018). Multiple-input configuration of isolated bidirectional DC–DC converter for power flow control in combinational battery storage.*IEEE Transaction on Industrial Informatics*, 14(1), 2–11.

Kumar, G.G., Sundaramoorthy, K., Athikkal, S., Karthikeyan, V., (2019).Dual input super boost DC-DC converter for solar powered electric vehicle.*IET Power Electronics*, 12(9),2276–2284.

Kumar, L., Jain, S., (2012).A novel dual input DC/DC converter topology.IEEE *International Conference on Power Electronics, Drives and Energy System*, 1–6.

Kumar, L., Jain, S., (2013). Multiple input DC / DC converter topology for hybrid energy system.*IET Power Electronics*, 6(8),1483–1501.

Kumaravel, S., Kumar, G.G., Veeranna, K., Karthikeyan, V., (2018).Novel Non isolated Modified Interleaved DC-DC Converter to Integrate ultracapacitor and Battery Sources for Electric Vehicle Application.*Proceedings of the National Power Systems Conference (NPSC).*

Maheswari Ellappan., Kavitha Anbukumar.,(2020). Compartive Analysis of ACM and GPWM Controllers in Continuous Input and Output Power Boost PFC Converter.*Journal of Control Engineering and Applied Informatics*,22(4),61-70.

Marikkannan, A., Manikandan, B.V., Mahesh Kumar, K., (2019).ZVS Asymmetrical PWM Full-bridge High Voltage Gain DC-DC Converter Controlled by ANFIS for Energy Harvesting Applications.*Journal of Control Engineering and Applied Informatics*,21(4),51-58.

Masoud Bahmanpour., Hamid Reza Koofigar., Majid Delshad., Mohammad Hasan Tosifian., (2019).Nonlinear control and Implementation of a Hybrid power system. *Journal of Control Engineering and Applied Informatics*,21(1),70-78.

Mudadla Dhananjaya., Swapnajit Pattnaik.,(2019).Design and Implementation of a Multi Input Single Output DC-DC Converter.*IEEE International Conference on Sustainable Energy Technology (ICSETS)*,194–199.

Omer Saleem Bhatti., Mohsin Rizwan., Muaaz Ahmad., (2018).Augmented Linear Quadratic Tracker for Enhanced Output-Voltage Control of DC-DC Buck Converter.*Journal of Control Engineering and Applied Informatics*,20(4),40-49.

Omer Saleem Bhatti., Umar Tabraiz Shami., Khalid Mahmood-ul-Hasan., Faisal Abbas., Samia Mahmood., (2019). Robust-Optimal Output-Voltage Control of Buck Converter using Fuzzy Adaptive Weighted Combination of Linear Feedback Controllers. *Journal of Control Engineering and Applied Informatics*,21(2),43-53.

Petru Dobra., Mirela Trusca., Daniel Moga., Dorin Petreus., (2007). Stability Aspects in DC-DC Converters Using PID Controller. *Journal of Control Engineering and Applied Informatics*,9(1),33-40.

Ridha Benadli., (2019).Improving Grid Connected hybrid generation system using an adaptive super-twisting sliding mode and predictive current control strategy. *Journal of Control Engineering and Applied Informatics*,21(2),64-75.

Sathishkumar, S., Rajkumar, M V., Kumar, SV., Maruthamuthu, M., Soundar, A., Kumaresann, A., (2017). A New Design for DC-DC Converter Topology with MISO for Renewable Energy Resources. *International Journal of Emerging Technology and Engineering Research*,5(4), 143–149.

Sivaprasad Athikkal., (2020). A Three input DC-DC converter for hybrid energy application. *International Journal of Electrical Engineering Technology*,11(4), 72-79.

Sivaprasad, A., Joseph, J., Kumaravel, S., Ashok, S., (2015). Design and analysis of a dual input DC-DC converter for hybrid electric vehicle. *IEEE International Conference Signal Process Informatics, Communication. and Energy System. (SPICES)*.

Subashini, N., Augusti Lindiya, S., Vijayarekha, K., Ramkumar, K., (2019). Performance Analysis of Sliding Mode Controlled Bridgeless Interleaved Boost Converter for Battery Charging Applications. *Journal of Control Engineering and Applied Informatics*, 21(3),20-30.

Sundaramoorthy Kumaravel., Ravishankar Achathuparambil Narayanankutty., Vemparala Seshagiri Rao., Ashok Sankar., (2019). Dual input dual output DC–DC converter for solar PV/battery/ultra capacitor powered electric vehicle application. *IET Power Electronics*, 12(13), 3351–3358.

Thakur, HS., Patel, R.N., (2019). Design and Development of Dual Input DC-DC Converter for Hybrid Energy System. *Journal of Circuits System and Computer*,28 (7),1-18.

Yasin, SA., Kumar, J., Kumar, Y., Athikkal, S., Peter, J., (2019). Analysis of A Dual Input DC-DC Converter Topology Based on SEPIC Configuration. *International Conference on Power Electronics Applications and Technology in Present Energy Scenario (PETPES)*.1-6.